SMAR 2015

3D-DIC for strain measurement in small scale GFRP RC specimens

Matteo Di Benedetti[1], Szymon Cholostiakow[1], Hamed Fergani[1], Emanuele Zappa[2], Alfredo Cigada[2], and Maurizio Guadagnini[1]

[1] The University of Sheffield, Sheffield, UK
[2] Politecnico di Milano, Milano, Italy

ABSTRACT: This paper presents preliminary results of a more extended experimental program on mechanical behaviour of fibre reinforced polymer (FRP) reinforced concrete (RC) beams. Two beams internally reinforced with GFRP bars are tested under a quasi-static four-point bending configuration. Displacement and strain values measured through the implementation of a three-dimensional digital image correlation (3D-DIC) system are compared to those recorded by well-established point wise transducers (strain gauges and potentiometers) and the quality of the full field, optical measurements is discussed and commented upon.

1 INTRODUCTION

In the past decade, digital image correlation (DIC), a contactless measuring technique for full-field strain estimation, has been increasingly spreading. However, despite its handiness, flexibility and density of measurable points, DIC can hardly compete in terms of resulting measurement accuracy with standard state-of-the-art strain measurements (typically performed using strain gauges). In particular, this represents a non-negligible issue when evaluating the strain distribution in brittle materials like concrete, where the resulting noise level in the collected data is generally too high (Mazzoleni 2013). In fact, while DIC has been successfully used in RC members to study cracking and deflections (Destrebecq et al. 2011 and Barris et al. 2014), very limited literature is available on quantitative strain analysis (Mazzoleni 2013).

The strain values estimated using DIC are a mathematical product of the measured displacement as shown in Sutton et al. (2009). Therefore, one of the main sources of error in the estimation of strains is the uncertainty associated with displacement measurements, which in turn is closely related to the quality of the speckle pattern (Pan et al. 2010). The latter can be assessed, among others, in terms of grey level histogram (Ghorbani et al. 2015; Destrebecq et al. 2011) and mean intensity factor (MIG), which represents a more effective global parameter (Pan et al.2010).

In this study, DIC is used to investigate the displacement and strain distribution within a predefined region of small-scale concrete specimens reinforced with GFRP bars and tested in four point bending. The DIC setup is designed to minimize the uncertainty in the measured in-plane displacement, which is achieved by using three-dimensional DIC and a fully controlled surface texturization. Preliminary results will be used to assess the quality of DIC displacement and strain estimates by comparing these with measurements obtained with well-established measurements techniques (i.e., strain gauges and potentiometers).

2 SPECIMENS AND MATERIALS

Two small-scale RC specimens are tested to study the effectiveness of full-field strain measurements using DIC. The test specimens are 110 mm wide, 150 mm deep and have a total length of 1200 mm (Figure 1 left). The longitudinal reinforcement consists of two glass fibre reinforced polymer (GFRP) bars in tension and two basalt fibre reinforced polymer (BFRP) bars in compression. The latter are mainly used to ease the building of the cages, since their contribution to ultimate capacity is negligible. GFRP shear links, equally spaced over the shear spans (e.g., every 100 mm), are used as shear reinforcement, while steel stirrups are used in proximity of both supports and loading points to prevent local crushing of concrete. Table 1 summarizes the material properties of the FRP reinforcements. The 28-day concrete compressive strength of 55 MPa is determined by testing three cubes according to BSI 2009.

3 TEST SETUP

3.1 Loading apparatus and point wise sensors

A four-point bending test is carried out on simply-supported specimens with a shear span of 333 mm and clear span of 1000 mm (Figure 1 left). Testing is performed using a hydraulic actuator with a maximum capacity of 1000 kN. The load is applied in displacement control at a rate of 1 mm/min. Quasi-static incremental loading cycles are performed at load levels inducing predefined level of strain in the tensile reinforcement (e.g., about 3000 με and 5000 με), before the specimens are loaded to failure. The applied load is measured using the internal force transducer in the actuator. Three potentiometers record deflections at the supports and at mid-span allowing for the computation of net deflection. Strain values at mid-span are measured using strain gauges bonded to the longitudinal GFRP bars and to the upper concrete surface in compression. An additional strain gauge is placed on the side face of the specimen at a distance of approximately 25 mm from the top compression face. The aforementioned measurements are used as benchmarks for those calculated with DIC.

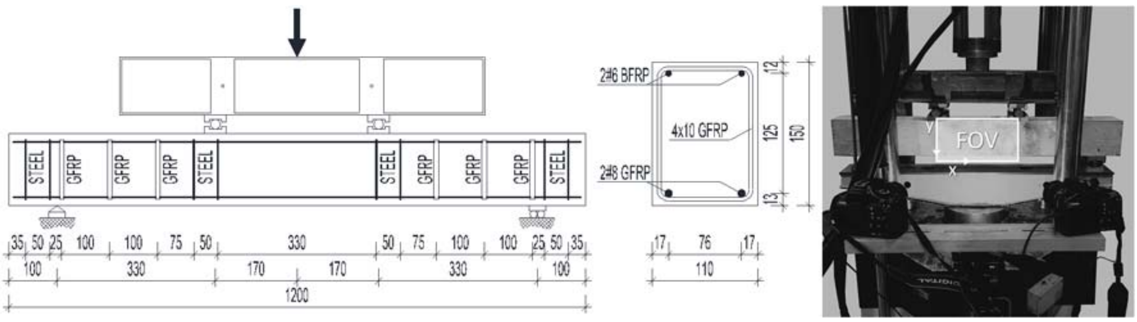

Figure 1. Test setup and internal reinforcement of the GFRP RC beams (left) and 3D-DIC test setup (right).

Table 1. Reinforcement material properties

Reinforcement		Modulus of Elasticity	Ultimate Strain	Ultimate Strength
Type	Material	E [GPa]	ε [%]	f [MPa]
Flexural	GFRP	56	2.7	1540
Shear	GFRP	45	1.8	800

3.2 DIC

The DIC setup is designed to try to minimize measurement uncertainty in order to obtain not only a displacement resolution similar to that of potentiometers, but also a strain resolution similar to that of the strain gauges. In order to achieve this objectives, two aspects are primarily taken into consideration: the DIC configuration and the speckles pattern.

3.2.1 DIC configuration

The 2D configuration, widely used for applications in RC, is easy to setup, implement, and analyse, but it cannot measure out of plane displacement. The importance of this limitation becomes immediately clear when the strain associated with out of plane displacement is estimated. As rule of thumb, a 1 mm out of plane displacement generates a strain equal to the inverse of the distance between camera and object. Therefore, for a distance of 500 mm, the strain will be 2000 µstrain. This means that a 2D configuration will estimate a fictitious strain of 2000 µstrain as part of the horizontal and vertical strains. Not knowing a priori the magnitude of the out of plane displacement, and being aware that this may lead to a strain measurement error similar to the strains in concrete, a 3D configuration, not affected by out of plane displacement, is employed. The setup of the 3D-DIC is shown in Figure 1 (right). In particular, the images are acquired with two CMOS digital cameras having a 4272×2848 pixel resolution (Canon EOS 1100D) and equipped with zoom lenses with F-number and focal length of 3.5-5.6 and 18-55 mm, respectively (Canon EF-S 18-55mm f/3.5-5.6 IS II). The cameras are rigidly connected 430 mm apart and mounted on a tripod. The stereo-vision system is positioned at 650 mm from the field of view (FOV). A light-emitting diode (LED) lamp is used to illuminate the measurement surface. The stereo-vision system is calibrated by taking images of a known pattern with different positions and orientations. The pattern included 14×12 dots with nominal diameter of 6 mm and centre-to-centre spacing of 15 mm. During the load test, the shutter is triggered remotely every 10 seconds by the DAQ recording the point wise sensors in order to synchronize all data.

3.2.2 Speckle pattern

In order to compare the DIC results with those measured with point wise sensors positioned at mid-span, the FOV is selected as an area of about 300×200 mm centred between the two loading points and extending below the specimen to take into account for the deflection at failure (Figure 1 right). This region is smoothed with sandpaper and cleaned before the application of the speckles. Two different methodologies to apply speckles are investigated. In Beam1, the speckles are spray-painted after whitewashing the specimen. This represents the easiest mean of application, but it is prone to locally increase measuring uncertainty as it offers limited control on speckle size and position. In Beam2, the pattern is generated using a laborious but highly accurate process. The pattern is first computer generated with randomly spaced speckles with a predefined nominal diameter and laser printed on a transfer paper. The speckles are then transferred to the beam by applying the paper on the concrete and gently rubbing it with a wet sponge. In order to minimize measurement uncertainty, the diameter of the speckle should be about 4-5 pixels (Lecompte et al. 2006, Zappa et al. 2014). In this study, given the resolution of the cameras and the size of the FOV, the speckles nominal diameter is 0.32 mm. The drawback of this methodology is that the speckles are not individually applied but they are part of an adhesive glossy film covering the beam. The effectiveness of these patterns will be analysed later in this manuscript in terms of grey level histogram and MIG.

3.2.3 Subset size

For this study, a subset of 91×91 pixels with a step of 30 pixel was used. Table 1 summarizes all the DIC parameters used in the following analysis. In the table, “object” refers to parameters calculated on the specimen plane (mm), while “image” refers to those calculated on the camera plane (pixels). Formulae to calculate these parameters are available in Sutton et al. (2009). Fixed parameters are the Image speckle dimension (5 pixels, on average by image inspection) for Beam1 and the Object speckle dimension (0.32 mm, computer designed pattern) for Beam2. Finally, the Image displacement accuracy was calculated as the standard deviation of the noise (Destrebecq et al. 2011) for pictures when no load was applied.

Table 1. DIC analysis parameters.

Parameter	Value		Units
	Beam 1	Beam 2	
Focal length	55		mm
FOV	300×200		mm
Recording resolution	4272×2848		pixels
Object-camera distance	650		mm
Magnification factor	13.53	13.09	pixels/mm
Subset Size	91×91		pixels
Overlap between contiguous subsets	61		pixels
Image displacement accuracy	0.0106	0.0117	pixels
Image speckle dimension	5	4.19	pixels
Object speckle dimension	0.37	0.32	mm
Spatial resolution	6.73	6.95	mm
Object displacement accuracy	0.0008	0.0009	mm

4 RESULTS AND DISCUSSION

The test results are presented in this section along with a comparison between the two speckle patterns and a discussion on the quality of displacement measurements and strain estimates using DIC.

4.1 Speckle pattern analysis

The speckles patterns of a representative region of 500×500 pixels as well as the associated grey level histograms are presented in Figure 2. Despite the two histograms do not have the bell-shaped distribution typical of a random grey levels pattern, they are still similar, suggesting comparable performance. In addition, the MIG is evaluated. The MIG is calculated on several subareas of an image recorded when no load is applied. The average MIG for Beam1 is 24 with standard deviation of 5.5 and coefficient of variation of 23%, while for Beam 2 it is 30 with standard deviation of 3.5 and coefficient of variation of 12%. The MIG values of both beams rank between good and very good if compared with the outcomes of Pan et al. (2010) research. Finally, the variability associated with the pattern of Beam2 is almost half of the one of Beam1, confirming the expected enhanced repeatability of computer generated patterns.

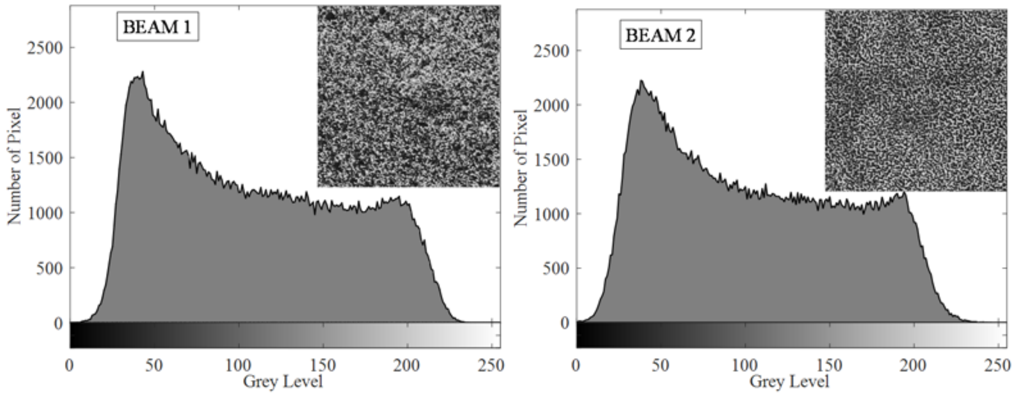

Figure 2. Speckle patterns and grey level histograms for a representative region of the two beams.

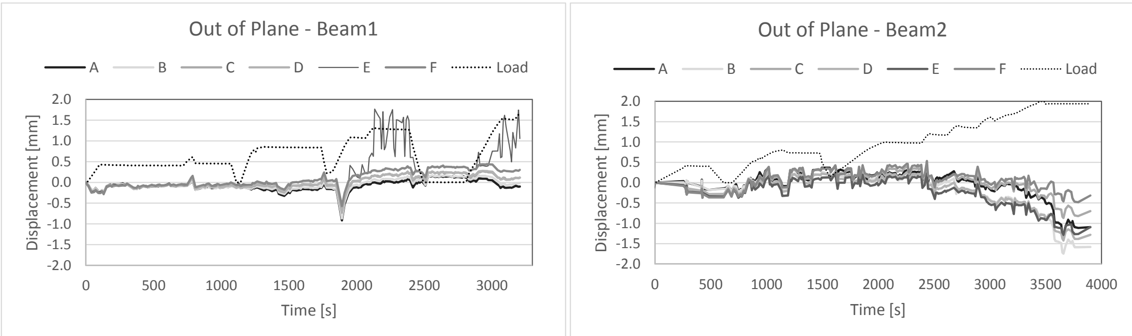

Figure 3. Out of plane displacement for Beam1 (left) and Beam2 (right).

4.2 Displacement

The use of 3D-DIC allows the analysis of vertical and horizontal displacements as well as the estimate of out of the plane measurements. The results of these analyses are presented below.

4.2.1 Out of plane

The first analysis uses out of plane displacement to evaluate the fictitious strain, which would have been introduced if a 2D-DIC were implemented. Figure 3 shows the out of plane displacement calculated for six points on both beams and plotted over time. These points (A, B, C, D, E, and F) are taken at the same subset coordinates (i.e., the couple [X_s, Y_s] is the number of subsets in the X and Y coordinates presented in Figure 1). These coordinates are [10, 10], [10, 50], [50, 10], [50, 50], [100, 50], and [100, 10], respectively. Finally, the dotted line represents the load trend over time.

The results show that for Beam2 the out of plane displacement is as high as 1.5 mm. This infers that, for an object-image distance of 650 mm, the fictitious strain measured by a 2D system would have been equal to 2300 µstrain. Since this strain is of the same order of magnitude of the concrete strain at crushing, the 2D-DIC could not have accurately measured strains, confirming that the only suitable choice for this study is a 3D setup.

4.2.2 Vertical displacement

Figure 4 shows, for both tests, the load plotted over the net deflection that was calculated as the difference between the deflection at mid-span and the average of those at the supports. The mid-span deflection was measured with a potentiometer (dark line) and with DIC (light line), while the deflection at supports was measured with potentiometers in both cases. The outcomes show that the deflection estimated with DIC agrees very well with that measured with the potentiometer.

4.2.3 Horizontal displacement

Full-field horizontal displacement, measured with DIC at the reinforcement bars level, is used to study the cracks pattern. Figure 5 plots the horizontal displacement of Beam1 over the physical position of the subset within the FOV. Different lines correspond to different load levels. On the right, the crack pattern on the side of Beam1 opposite to the one examined with DIC is presented.

Figure 5 (left) shows two discontinuities, at about 160 mm of the FOV, that are the result of the lack of correlation encountered by the DIC software where no speckles pattern was applied because of the presence of strain gauges cables. The scatter in the data on the right side of the FOV can be attributed to the fact that such discontinuities occur in proximity of a crack and that a sudden change in the out of plane displacement occurs (Figure 3 left, at 2000 s). On the left side of these discontinuities, DIC can locate the crack in the form of a step in the horizontal displacement. However, acceptable accuracy is limited for load values up to about 25 kN. In this range of loads, the crack width can also be estimated as the amplitude of the step in the horizontal displacement curve. In particular, the crack width measured at 20 kN is 0.4 mm, which is twice the one measured with an optical magnifier for the same crack but on the opposite side of the beam. Such discrepancy can be attributed to the fact that the measurements were carried out on opposite sides and that, for the considered load, the out of plane displacement is compatible with the crack width, thus affecting the quality of the calculated values.

Keeping in mind the poor accuracy of the results obtained at the two ends of the FOV, only the portion within the two cracks will be considered for the strain analysis. The same considerations also apply to the analyses performed on Beam2.

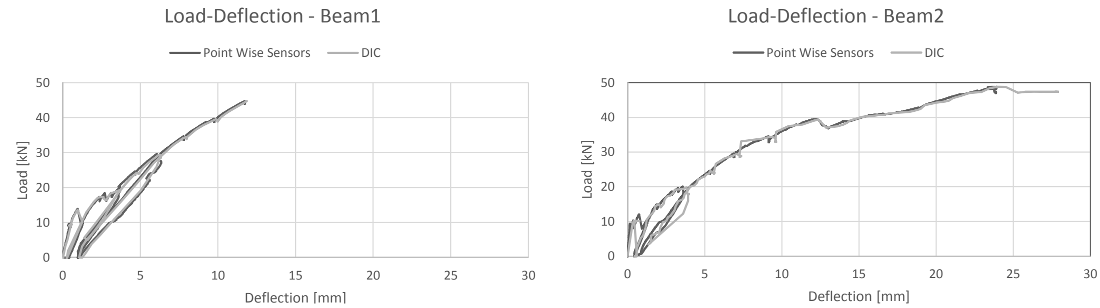

Figure 4. Load-deflection curves for Beam1 (left) and Beam2 (right).

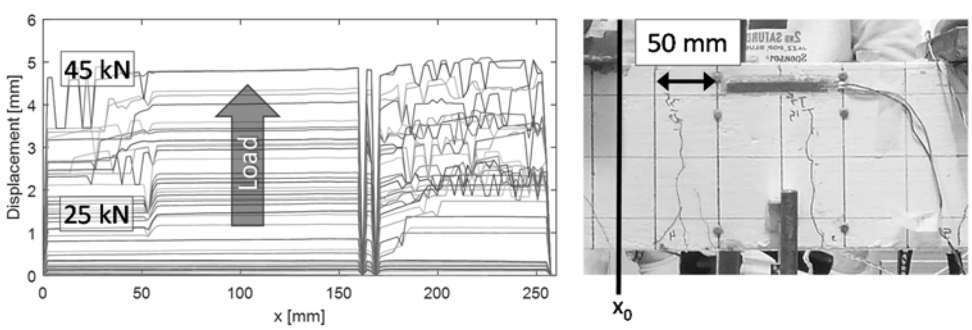

Figure 5. Beam1: horizontal displacement of for increasing load levels (left) and crack pattern (right).

4.3 Strain

In this section, strain results are presented and the agreement between DIC and strain gauges measurements is assessed. Figure 6 shows, for both beams, the full-field strains estimated with DIC for images taken at a similar load level (40 kN). For clarity, two contour plots are used to show only compressive strain (A and B) and tensile strain (C and D), respectively. In addition, the regions that will not be considered in the strain analysis are shaded and crossed. Before further discussing the results, it should be noted that strain gauges in tension are placed on the reinforcing bars and are expected to measure higher strain values than those estimated with DIC from the analysis of surface deformation. Conversely, strain gauges in compression measure strains on the concrete surface, and thus will be used to directly benchmark the values estimated with DIC.

The analysis on Beam1 (sprayed speckle pattern) yields qualitatively good results as the strain in compression and tension correctly describe the physical behavior of the beam. In fact, white and colored regions clearly define the compression (top) and tension (bottom) zone. In addition, the neutral axis (boundary between white and colors) falls in between the two cracks up to values that are compatible with those analytically calculated (19 mm). On the other hand, the maximum local compressive strain is estimated equal to 1090 $\mu\varepsilon$, which is much lower than the value recorded with strain gauges (1750 $\mu\varepsilon$). In Beam2 (computer generated speckle pattern), the overall strain distribution does not correctly represents the behavior of the beam, showing that the cross-sections within the two cracks are all in compression (Figure 6 B). The estimated strains, in the portion of the beam that acts in tension, are compressive strains, though relatively small (less than 700 $\mu\varepsilon$ in compression). This could be due to a partial debonding and consequent relaxation of the film where the speckles are printed. Conversely, the maximum compressive strain at the top of the beam is equal to 1850 $\mu\varepsilon$ and agrees well with the values obtained from strain gauges (1840 $\mu\varepsilon$).

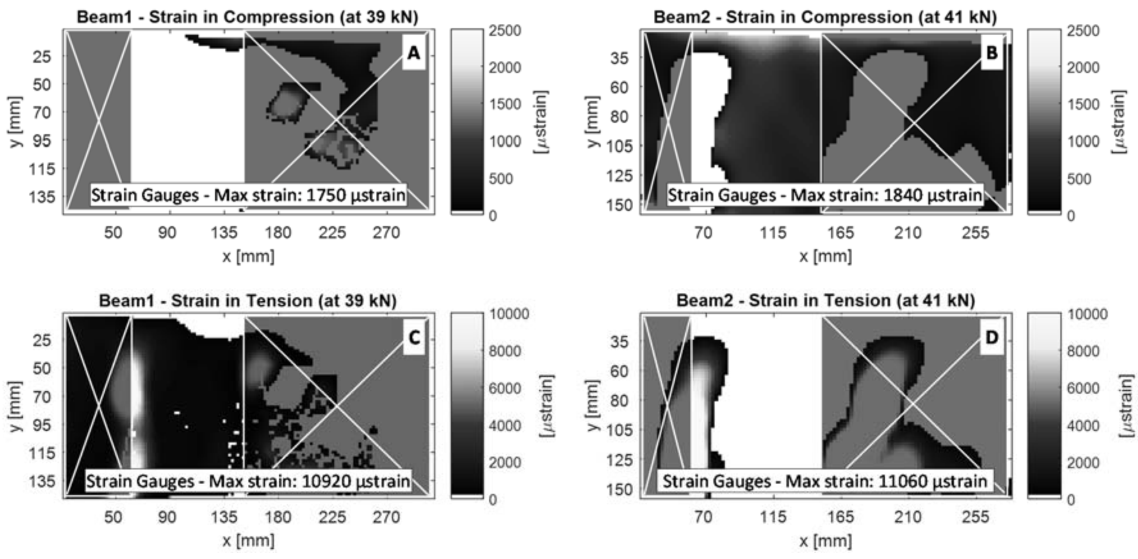

Figure 6. Full-field strains estimated with DIC for Beam1 (A and C) and Beam2 (B and D)

5 CONCLUSIONS

In this study, small-scale GFRP RC beams are load-tested to assess the effectiveness of DIC to measure displacement and strain in RC members. Based on the discussion presented above, the following conclusions can be drawn:

1. The computer generated speckle pattern, as well as the sprayed one, have high MIG values, and therefore are of high quality.
2. 3D-DIC is the only viable setup when out of plane displacement may occur and reliable full-field strain estimates are required.
3. Vertical displacements measured with DIC agree well with measurements recorded with potentiometers.
4. Crack width can be estimated with sufficient accuracy using DIC, but limitations apply in terms of out of plane displacement and position within the field of vision.
5. Strain values in the compression region of the beam are more accurately estimated when using the computer generated speckle pattern.
6. Neutral axis position is estimated with sufficient accuracy only when using the sprayed speckle pattern.

The contrasting results obtained for the two beams in terms of strain underlines the complexity of the interpretation of the DIC results. A simple and novel way of transferring a computer generated speckle pattern on the surface of the test specimens was explored. Additional tests, however, are needed to confirm the effectiveness of this technique.

6 ACKNOWLEDGEMENTS

The authors would like to acknowledge the financial support offered by the European Union, which funded the Marie Curie Network endure under the FP7-PEOPLE-2013-ITN Programme (contract number: 607851).

7 REFERENCES

BSI. 2009. *Testing hardened concrete. Compressive strength of test specimens (BS EN 12390-3:2009)*, British Standard Institution.

Destrebecq, J.F., E. Toussaint, and E. Ferrier, 2011. Analysis of Cracks and Deformations in a Full Scale Reinforced Concrete Beam Using a Digital Image Correlation Technique, *Experimental Mechanics*, 51, 879–890.

Barris, C., I. Vilanova, L. Torres, C. Mias, and A. Massaguer, 2014. Analysis of Cracking of GFRP RC Beams with a Digital Image Correlation System, *Proc. CICE 2014: The 7th International Conference on FRP Composites in Civil Engineering*, 20-22 August, Vancouver, Canada.

Ghorbani, R., F. Matta, and M.A. Sutton, 2015. Full-Field Deformation Measurement and Crack Mapping on Confined Masonry Walls Using Digital Image Correlation, *Experimental Mechanics*, 55(1): 227-243.

Lecompte, D., H. Sol, J. Vantomme, and A. Habraken, 2006. Analysis of speckle patterns for deformation measurements by digital image correlation, *Proc. SPIE 6341, Speckle06: Speckles, From Grains to Flowers*, 63410E, Nimes, France.

Mazzoleni, P. 2013. *Uncertainty estimation and reduction in digital image correlation measurements*, Doctoral Dissertation, Politecnico di Milano, Italy.

Pan, B., L. Zixing, and X. Huimin, 2010. Mean intensity gradient: An effective global parameter for quality assessment of the speckle patterns used in digital image correlation, *Optics and Lasers in Engineering*, 48, 469–477.

Sutton, MA, Orteu, JJ, and Schreier, HW. 2009. *Image Correlation for Shape, Motion and Deformation Measurements - Basic Concepts, Theory and Applications.* New York: Springer Science+Business Media.

Zappa, E., P. Mazzoleni, and A. Matinmanesh, 2014. Uncertainty assessment of digital image correlation method in dynamic applications, *Optics and Lasers in Engineering*, 56, 140-151.